

Article

Spin-Crossover Behavior of Hofmann-Type-Like Complex $\text{Fe}(4,4'\text{-bipyridine})\text{Ni}(\text{CN})_4 \cdot n\text{H}_2\text{O}$ Depending on Guest Species

Kazumasa Hosoya ^{1,†}, Shin-ichi Nishikiori ^{1,†}, Masashi Takahashi ^{2,3,†} and Takafumi Kitazawa ^{2,3,*}

¹ Department of Basic Science, Graduate School of Arts and Sciences, the University of Tokyo, 3-8-1, Komaba, Meguro-ku, Tokyo 153-8902, Japan; hosoyakazumasa@gmail.com (K.H.); cnskor@mail.ecc.u-tokyo.ac.jp (S.N.)

² Department of Chemistry, Faculty of Science, Toho University, 2-2-1 Miyama, Funabashi, Chiba 274-8510, Japan; takahasi@chem.sci.toho-u.ac.jp

³ Research Centre for Materials with Integrated Properties, Toho University, 2-2-1 Miyama, Funabashi, Chiba 274-8510, Japan

* Correspondence: kitazawa@chem.sci.toho-u.ac.jp; Tel.: +81-47-472-5077; Fax: +81-47-475-5077

† These authors contributed equally to this work.

Academic Editors: Guillem Aromí and José Antonio Real

Received: 7 January 2016; Accepted: 1 February 2016; Published: 16 February 2016

Abstract: A newly prepared metal complex $\text{Fe}(4,4'\text{-bipyridine})\text{Ni}(\text{CN})_4 \cdot n\text{H}_2\text{O}$, which was estimated to have a structure similar to the Hofmann-type clathrate host, changed its color from orange to deep orange and yellow on exposure to ethanol and acetone vapor, respectively, and the respective samples showed thermally induced two-step and one-step spin transitions.

Keywords: spin-crossover; vapochromism; guest inclusion; isotope effect

1. Introduction

Spin-crossover Fe^{II} complexes are a promising source for new functional molecular switches because they can alternate between a high-spin (HS) and a low-spin (LS) state depending on the circumstances and show variations in magnetism, color and structure [1–6]. Many spin-crossover Fe^{II} complexes, especially those with polymeric structures, have been intensively studied because their polymeric linked structures enhance cooperative effects which work among the spin-crossover species resulting in spin transitions with hysteresis [7–17]. If such Fe^{II} complexes gain another physical or chemical property besides spin-crossover, they would be even more fascinating as multi-functional materials. We now report such an example, an Fe^{II} complex that shows a spin transition and vapochromism.

As 2D polymeric structure complexes, the Hofmann-type clathrate host complexes $\text{M}^{\text{II}}(\text{NH}_3)_2\text{M}'^{\text{II}}(\text{CN})_4$ ($\text{M} = \text{Mn}, \text{Fe}, \text{Co}, \text{Ni}, \text{Cd}$; $\text{M}' = \text{Ni}, \text{Pd}, \text{Pt}$) are known, in which octahedral M^{II} and square planar M'^{II} are alternately linked by cyanide bridges to form a 2D $[\text{M}'^{\text{II}}(\text{CN})_4\text{M}^{\text{II}}]_{\infty}$ bimetallic cyanide network [18–21]. At M^{II} , the four N ends of the cyanide bridges and two amines coordinate to the four equatorial and two axial sites of M^{II} , respectively, to complete an $\text{M}^{\text{II}}\text{N}_6$ octahedral coordination sphere. In the Hofmann-type clathrate, the cyanide networks are stacked to form a layered structure that works as a host for small organic molecules such as benzene, pyrrole, aniline, *etc.* As a modification of this complex, Hofmann-pyridine-type complexes $\text{M}^{\text{II}}(\text{py})_2\text{Ni}^{\text{II}}(\text{CN})_4$ ($\text{py} = \text{pyridine}$) are known [22–24]. These have no ability as a clathrate host but, in the case of $\text{M} = \text{Fe}$, it shows a spin transition with thermal hysteresis [25]. Further structural development from a 2D to a 3D structure by replacing the unidentate pyridine with bidentate pyrazine generated the complex

$\text{Fe}^{\text{II}}(\text{pyrazine})\text{M}^{\text{II}}(\text{CN})_4 \cdot n\text{H}_2\text{O}$, where a spin transition with a higher transition temperature and a wider hysteresis loop were achieved [26–28]. Based on this history, we tried to synthesize a new Hofmann-type-like Fe^{II} complex using a larger bidentate ligand 4,4'-bipyridine (bpy), expecting the resultant complex to function as a host and also possess spin-crossover properties.

2. Results and Discussion

Our new complex $\text{Fe}^{\text{II}}(\text{bpy})\text{Ni}^{\text{II}}(\text{CN})_4 \cdot n\text{H}_2\text{O}$ ($n = 2.5$)(**1**) was obtained as powder from a mixture of Mohr's salt, $\text{K}_2[\text{Ni}(\text{CN})_4] \cdot \text{H}_2\text{O}$, 4,4'-bipyridine (bpy), water and acetone. Its crystallinity was poor and no crystalline sample has been obtained. Because the single crystal X-ray diffraction method was inapplicable, the structural information was obtained from indirect methods such as EXAFS (Extended X-ray Absorption Fine Structure), IR spectroscopy and powder X-ray diffraction.

While Temperature-dependent EXAFS study for spin crossover complex $\text{Fe}(\text{py})\text{Ni}(\text{CN})_4$ was reported [29], the information about the coordination structures of Fe^{II} and Ni^{II} was obtained from EXAFS spectra. The EXAFS functions of **1** and a Hofmann-type-like complex $\text{Fe}(\text{py})_2\text{Ni}(\text{CN})_4$, whose crystal structure is shown in Figure 1a, after the Fourier conversion were shown in Figure 2. Similarity between **1** and $\text{Fe}(\text{py})_2\text{Ni}(\text{CN})_4$ in Fe K-edge and Ni K-edge EXAFS spectra are clear. These findings strongly suggest the coordination structures of Fe^{II} and Ni^{II} atoms of both compounds are very similar. The two intense peaks of **1** in the Ni K-edge EXAFS spectra come from the multiple-scattering from the linearly arranged Ni with a square planar form, C and N atoms, namely Ni-C-N linear linkage [29,30]. The third small peak around *ca.* 4.5 Å arise from the Fe atom bound to the N end of the Ni-C-N linkage. The figure seeing the linkage from the Fe end is the Fe K-edge EXAFS spectrum. The remarkable three peaks in the Fe K-edge EXAFS spectrum come from the linear arrangement of Fe-N-C-Ni linkage. The Fe has an octahedral configuration by six atoms so that the first peak is more intense than that in the Ni K-edge spectrum. These situation well agree with the network structure of the Hofmann-type host complex $\text{Fe}(\text{ligand})_2\text{Ni}(\text{CN})_4$ as shown in Figure 1b. The EXAFS spectra of **1** which are almost identical to those of $\text{Fe}(\text{py})_2\text{Ni}(\text{CN})_4$ strongly suggest that **1** has the net structure of the Hofmann-type host complex.

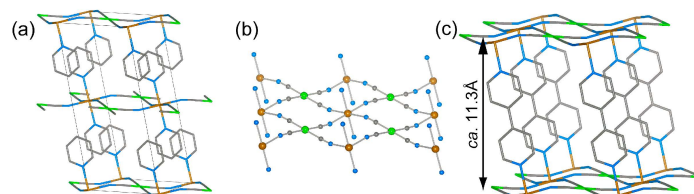


Figure 1. (a) Crystal structure of $\text{Fe}(\text{py})_2\text{Ni}(\text{CN})_4$ [25]; (b) the network structure of the Hofmann-type host complex $\text{M}(\text{ligand})_2\text{Ni}(\text{CN})_4$; and (c) a structure estimated for $\text{Fe}(\text{bpy})\text{Ni}(\text{CN})_4 \cdot n\text{H}_2\text{O}$ ($n = 2.5$)(**1**). (orange: Fe^{II} , green: Ni^{II} , gray: C; blue: N; H atoms are omitted for clarity.)

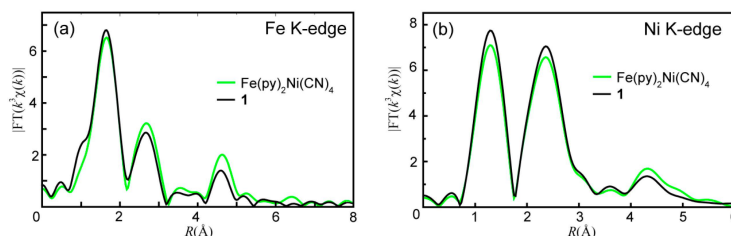


Figure 2. (a) Fe K-edge and (b) Ni K-edge Extended X-ray Absorption Fine Structure (EXAFS) spectra of **1** and $\text{Fe}(\text{py})_2\text{Ni}(\text{CN})_4$.

In IR spectrum of **1**, a sharp absorption band was observed at 2153 cm^{-1} (Figure S1), assignable to the stretching mode of cyanide. This finding shows that there is only one kind of cyanide ligand in

1. Considering the results of the EXAFS spectra all cyanides in **1** work as bridging ligands to form a bimetallic cyanide network. This is the picture of the cyanide ligand seen in the Hofmann-type host complexes [22,31,32].

In many Hofmann-type-like complexes, a characteristic powder X-ray diffraction pattern coming from a well-regulated layered structure of the cyanide networks is observed [33]. The intensity of the powder pattern measured for **1** was rather weak. However, a series of diffraction peaks suggesting a layered structure with a space distance of *ca.* 11.3 Å was observed (Figure S2). This distance agrees with that of 11.5 Å observed in a known spin cross over (SCO) complex [Fe(bpy)(biim)₂](ClO₄)₂·2C₂H₅OH (biim = 2-(2-pyridyl)imidazole)), which contains bpy working as a bridge between two Fe(II) atoms [34]. Based on the above information, the basic structure of **1** is the layered structure similar to that of the Hofmann-type host complex and the layers are linked by bridging bpy ligands. In this structure, there is void space between the layers and the bpy ligands acting as pillars supporting the layers. Figure 1c illustrates a structure estimated for **1** from the above information. The water molecules are trapped in this space and there is a possibility that the water molecules are replaceable with other molecules.

1 showed vapochromic behavior [35–41]. The orange powder of **1** displayed a color change on exposure to certain organic compounds, such as ethanol, acetone, 2-propanol, *etc.*, in the gas phase. In this paper, we report the cases of ethanol and acetone. From the contact of **1** with ethanol and acetone vapor at room temperature and under ambient pressure, deep orange (**2**) and yellow (**3**) powders were obtained, respectively. Accompanying these color changes, the weight of **1** increased by 5.0%–8.0% and 10%–30%, respectively. These color changes were reversible. **2** and **3** were very labile in a guest-free atmosphere. They quickly released the guests and returned to the orange powder **1**. Diffuse reflectance spectra of **1**, **2** and **3** are shown in Figure 3. Although clear change was observed visually between **1** and **2**, the difference in diffuse reflectance spectrum between them was little. Between **1** and **3**, clear change was recognized in their spectra and the spectrum of **3** returned to that of **1** by standing **3** in air. These findings suggest that the coordination environment in **1** receives some influence from the absorption of acetone molecules.

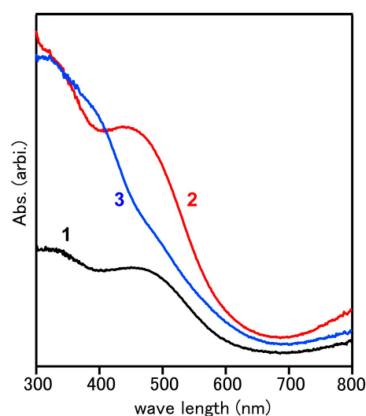


Figure 3. Diffuse reflectance spectra of **1**, **2** and **3**.

Magnetic susceptibility measurements revealed that **1** did not show any spin-crossover phenomenon but the guest-containing samples **2** and **3** did show spin-crossover. The $\chi_M T$ vs. T plots are shown in Figure 4a. In the range between 50 K and 300 K, the $\chi_M T$ value of **1** was almost constant at *ca.* 3.3 emu K mol⁻¹. This value is close to the expected value of 3.0 emu K mol⁻¹ for a Fe^{II} HS ($S = 2$) state. This confirms that the Ni^{II} maintains the diamagnetic square planar [Ni(CN)₄]²⁻ moiety, which is the structural base of Hofmann-type-like cyanide networks [18–21]. In contrast to **1**, **2** showed a two-step spin transition with thermal hysteresis, the critical temperatures of which on cooling ($T_C \downarrow$) were 213 and 187 K, and on warming ($T_C \uparrow$) were 223 and 197 K. These T_C values are close to those observed in the Hofmann-pyridine-type complex Fe(py)₂Ni(CN)₄. [25,42] In **3**, a spin transition was

observed as a one-step transition with hysteresis, the $T_{C\downarrow}$ and $T_{C\uparrow}$ of which were 125 and 145 K, respectively. The T_C values of **3** are considerably lower than those of $\text{Fe}(\text{py})_2\text{Ni}(\text{CN})_4$. In both cases, the spin transitions were not complete. Below 100 K, 20%–25% of Fe^{II} remained in the HS state.

Figure 4b,c shows the results of samples processed with deuterated ethanol ($\text{C}_2\text{D}_5\text{OD}$) and acetone ($(\text{CD}_3)_2\text{CO}$). The sample including $\text{C}_2\text{D}_5\text{OD}$ showed small shift to higher temperature region as often observed in deuterated SCO complexes. However, in the sample containing $(\text{CD}_3)_2\text{CO}$, a remarkable increase in the hysteresis width was observed [42]. Such increase in hysteresis width coming from deuteration is rare [42]. Table 1 lists the transition temperatures including those obtained from the deuterated samples. In the case of the influence of hydrogen bonding on the hysteresis width in iron(II) spin crossover complexes, Weber *et al.* reported an increase of hysteresis width after deuteration [43]. This is much more pronounced and remarkable for the presence case with $(\text{CH}_3)_2\text{CO}$.

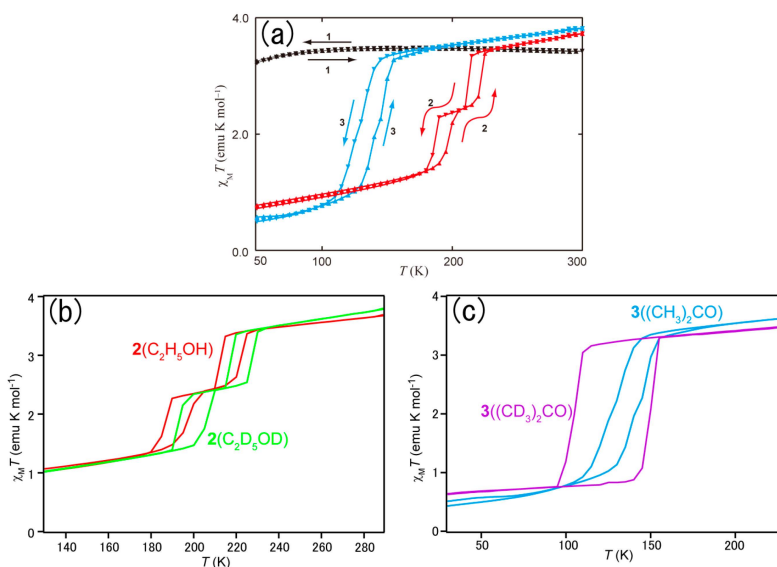


Figure 4. $\chi_{\text{M}}T$ vs. T plots (a) for **1**, **2**, and **3**; (b) for **2** containing $\text{C}_2\text{H}_5\text{OH}$ and $\text{C}_2\text{D}_5\text{OD}$; and (c) **3** containing $(\text{CH}_3)_2\text{CO}$ and $(\text{CD}_3)_2\text{CO}$.

Table 1. Spin transition temperatures of **2** and **3** determined by magnetic susceptibility measurements.

Sample	$T_{c\downarrow}^a$ (K)	$T_{c\uparrow}^b$ (K)	Δ^c (K)	$T_{c\downarrow}^a$ (K)	$T_{c\uparrow}^b$ (K)	Δ^c (K)
$2(\text{C}_2\text{H}_5\text{OH})$	187	197	10	213	223	10
$2(\text{C}_2\text{D}_5\text{OD})$	190	205	10	215	230	10
$3((\text{CH}_3)_2\text{CO})$	125	145	20	-	-	-
$3((\text{CD}_3)_2\text{CO})$	103	148	45	-	-	-

a and *b*: transition temperature in the heating and cooling mode, respectively. *c*: hysteresis width.

The spin states of **1**, **2** and **3** are confirmed by ^{57}Fe Mössbauer spectra shown in Figure 5. Mössbauer parameters obtained from the spectra are listed in Table 2. In all spectra, two kinds of absorption, one major and one minor, were observed. The main absorption of **1** comprised quadrupole doublets corresponding to Fe^{II} in the HS state, the isomer shift (δ) and quadrupole splitting (ΔE_{Q}) of which were $1.00(3) \text{ mm s}^{-1}$ and $0.63(3) \text{ mm s}^{-1}$ at 298 K, and $1.13(3) \text{ mm s}^{-1}$ and $1.10(3) \text{ mm s}^{-1}$ at 77 K, respectively. No remarkable change was observed between the spectra of **1** at 298 K and 77 K. In **2**, the dominant absorption observed at 298 K was a doublet with δ of $1.04(2) \text{ mm s}^{-1}$ and ΔE_{Q} of $0.69(2) \text{ mm s}^{-1}$, which corresponds to Fe^{II} in the HS state. At 77 K this signal almost completely converted into an absorption peak assignable to Fe^{II} in the LS state with δ of $0.52(2) \text{ mm s}^{-1}$ and ΔE_{Q} of $0.31(2) \text{ mm s}^{-1}$. The spectral change observed in **3** was similar to the case of **2**. The doublet of the major absorption at

room temperature, whose δ and ΔE_Q were 1.070(1) mm s⁻¹ and 1.190(2) mm s⁻¹, respectively, converted into a singlet peak with δ of 0.490(2) mm s⁻¹ and ΔE_Q of 0.217(6) mm s⁻¹ at 77 K.

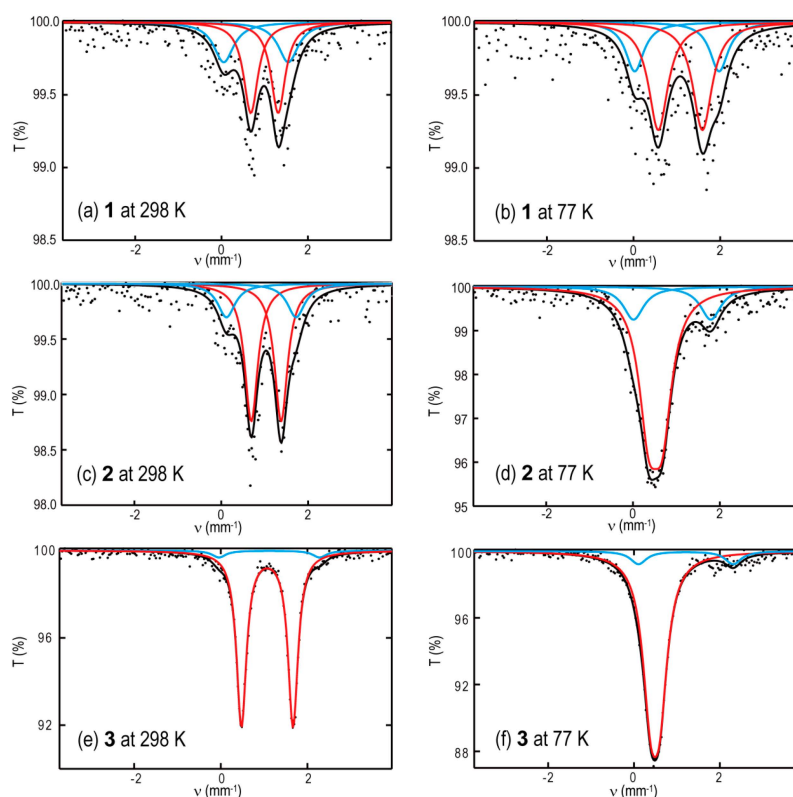


Figure 5. Mössbauer spectra of **1**, **2** and **3** at 298 K and 77 K: (a,b) **1** at 298 K and 77 K; (c,d) **2** at 298 K and 77 K; and (e,f): **3** at 298 K and 77 K. The red and the blue line show the major and the minor component, respectively. The black line shows the sum of both components.

Table 2. Mössbauer parameters for **1**, **2** and **3**.

Compound	Temp (K)	Signal	State	δ (mm s ⁻¹)	ΔE_Q (mm s ⁻¹)	Area (%)
1	298	major	HS	1.00(3)	0.63(3)	62
		minor	HS	0.80(3)	1.50(3)	38
	77	major	HS	1.13(3)	1.10(3)	71
		minor	HS	1.02(3)	1.96(3)	29
2	298	major	HS	1.04(2)	0.69(2)	75
		minor	HS	0.92(2)	1.60(2)	25
	77	major	LS	0.52(2)	0.31(2)	78
		minor	HS	0.90(2)	1.79(2)	22
3	298	major	HS	1.07(1)	1.19(1)	95
		minor	HS	1.12(3)	2.31(7)	5
	77	major	LS	0.49(1)	0.22(1)	90
		minor	HS	1.07(3)	1.97(5)	10

HS: High Spin; LS: Low Spin; δ : isomer shift; Δ : quadrupole splitting.

These observations on the major components agree with the spin transition observed in the magnetic susceptibility measurement. Comparing the Mössbauer parameters with those obtained in Fe(py)₂Ni(CN)₄ [25,42] and its related complexes [44–51], this major signal is considered to come

from the octahedral $\text{Fe}^{\text{II}}\text{N}_6$ species in the cyanide network. On the other hand, the minor signals, which always appeared as a doublet assignable to Fe^{II} in the HS state in **1**, **2**, and **3**, showed no large change over all measurements. This invariant HS state corresponds to the residual magnetization observed in the $\chi_{\text{M}}T$ vs T plot of **2**. Its larger ΔE_{Q} value suggests that the coordination environment around the HS Fe^{II} is more distorted than that of the major component. Although one imaginable case is that some Fe^{II} ions are coordinated by H_2O molecules, no effective method for its confirmation is available. The whole spectral intensity of **1** was weak. On the other hand, in the spectra of **2** and **3**, their intensities were rather strong. The absorption of the guest molecules is considered to improve the stiffness of the host lattice and recoilless fraction.

3. Experimental Section

The new complex $\text{Fe}^{\text{II}}(\text{bpy})\text{Ni}^{\text{II}}(\text{CN})_4 \cdot n\text{H}_2\text{O}$ (**1**) was obtained by the following method. Acetone (30 mL) was added to a mixture of 4,4'-bipyridine (bpy, 0.16 g, 10 mmol), Mohr's salt (0.39 g, 10 mmol) and $\text{K}_2[\text{Ni}(\text{CN})_4] \cdot \text{H}_2\text{O}$ (0.26 g, 10 mmol). After bpy was dissolved, water (30 mL) was poured into the mixture with stirring. Immediately a yellow precipitate appeared. After 30 min stirring, the precipitate was filtered, washed with water and acetone successively, and dried well using an aspirator. In this process the color of the precipitate changed from yellow to orange. The final product, **1**, was obtained as an orange powder. Elemental analysis supported a Hofmann-type-like formula of $\text{Fe}(\text{bpy})\text{Ni}(\text{CN})_4 \cdot n\text{H}_2\text{O}$ ($n = 2.5$). Found: C, 39.71%; H, 3.05%; N, 19.89%; Fe, 13.11%; Ni, 13.88%. Calc. for $\text{C}_{14}\text{H}_{13}\text{N}_6\text{O}_{2.5}\text{FeNi}$: C, 40.05%; H, 3.12%; N, 20.02%; Fe, 13.30%; Ni, 13.98%.

IR spectrum of **1** was measured by the Nujol mull method using JASCO FTIR-350 spectrometer (JASCO Corp., Hachioji, Tokyo, Japan). Powder X-ray diffraction pattern of **1** was measured using a Rigaku Multi-Flex diffractometer (Rigaku Corp., Akishima, Tokyo, Japan) with graphite monochromated $\text{Cu K}\alpha$ radiation ($\lambda = 1.5406 \text{ \AA}$). Thermogravimetric analysis (TG) was carried out using TA instruments TGA 2950 thermobalance (TA Instruments, New Castle, DE, USA) at 10 K min^{-1} scan rate under N_2 gas flow. The results of IR, XRD and TG are shown in Figures S1, S2 and S3, respectively.

Diffuse reflectance spectra of **1**, **2** and **3** were measured on a JASCO V-570 UV/VIS spectrometer (JASCO Corp., Hachioji, Tokyo, Japan) equipped with a JASCO ISN-470 integrating sphere (JASCO Corp., Hachioji, Tokyo, Japan) at room temperature. The powder samples were diluted with BaSO_4 powder and sealed in a cell with quartz window.

The Fe and Ni K-edge EXAFS spectra of **1** and $\text{Fe}(\text{py})_2\text{Ni}(\text{CN})_4$ were measured at BL-9C station of the Photon Factory (PF) in High Energy Accelerator Research Organization (KEK, Tsukuba, Japan). The powder samples were pressed to disks and the measurements were carried out in the transmission mode at ambient temperature. The radiation was monochromatized with Si(111) double crystals. The spectra were recorded over the range between 6604.2–8205.2 eV for Fe K-edge spectra and 7826.7–9425.7 eV for Ni K-edge spectra. The data reduction from the absorption spectra to EXAFS functions of $k^3\chi(k)$ and Fourier transformed functions $\text{FT} |k^3\chi(k)|$ were carried out using the program Athena/Ifeffit (Ver. 0.8.061, CARS(the Consortium for Advanced Radiation Sources), Chicago, IL, USA, 2009) [52]. For the spectra of $\text{Fe}(\text{py})_2\text{Ni}(\text{CN})_4$ the curve fitting was performed based on the structural information [25] over the real space range of $R = 1\text{--}8 \text{ \AA}$ using the program Artemis/Ifeffit [52] and FEFF8 (Ver. 8.40, FEFF Project, Seattle, WA, USA, 2008) [53], including multiple-scattering paths. This analysis confirmed that the characteristic three peaks come from the linear atom arrangements of Fe-N-C-Ni and Ni-C-N-Fe as mentioned in the Result and Discussion Section. The fitting results and parameters used are shown in Figure S4 and Table S1, respectively.

Magnetic susceptibility measurements were carried out for **1**, **2**, and **3** between 10 and 300 K using a Quantum Design MPMS-5 superconducting quantum interference device (SQUID) magnetometer (Quantum Design Inc., San Diego, CA, USA). The samples of **2** and **3** were sealed into an Al cell to prevent the release of the guest molecules. External magnetic field of 1000 Oe was applied and scan rate of 0.5 K min^{-1} was used.

^{57}Fe Mössbauer experiments were carried out on powder samples of **1**, **2** and **3**, which were sealed into a cell made of poly(methyl methacrylate), at 298 K and 77 K using a Wissel Mössbauer spectrometer system consisting of an MDU-1200 driving unit (Wissenschaftliche Elektronik GmbH, Starnberg, Germany) and an MVT-100 velocity transducer (Wissenschaftliche Elektronik GmbH, Starnberg, Germany), incorporating with a Seiko Model 7800 multi-channel analyzer (Seiko EG&G Co., Ltd., Chuo-ku, Tokyo, Japan). The temperature control of the samples was done with a Heli-Tan LT-3 gas-flow cryostat (Advanced Research System Inc., Allentown, PA, USA) with a 9620 digital temperature controller (Science Instruments, Inc., West Palm Beach, FL, USA) from Scientific Instruments, and the $^{57}\text{Co}(\text{Rh})$ source (Ritverc GmbH, Petersburg, Russia) was kept at room temperature. δ values are given with respect to α -iron foil at room temperature.

4. Conclusions

Spin-crossover phenomena depending on guest inclusion are already known in several Fe^{II} complexes [54–64]. Among them, this case, $\text{Fe}^{\text{II}}(\text{bpy})\text{Ni}^{\text{II}}(\text{CN})_4 \cdot n\text{H}_2\text{O}$ ($n = 2.5$), is unique in the simultaneity of vapochromism and spin transition. Moreover, the appearance of the spin transition strongly depends on the normal and deuterated guest species.

Acknowledgments: The Extended X-ray Absorption Fine Structure (EXAFS) measurements were performed under the approval of the Photon Factory Program Advisory Committee, PF-PAC No. 2008P006. We wish to thank Norimichi Kojima and Masaya Enomoto (Graduate School of Arts and Sciences, University of Tokyo) for their technical support for measuring magnetic susceptibility, and Yoshihiro Okamoto (Japan Atomic Energy Agency-Tokai) for his support for measuring and analyzing EXAFS spectra. This work was partly supported by MEXT (Ministry of Education, Culture, Sports, Science and Technology, Japan)-Supported Program for the Strategic Research Foundation at Private Universities, 2012–2016. This work was also partly supported by Japan Society for the Promotion Science (JSPS) KAKENHI Grant Number 15K05485.

Author Contributions: Kazumasa Hosoya and Shin-ichi Nishikiori conceived and designed the experiments; Kazumasa Hosoya and Takafumi Kitazawa measured and analyzed magnetic susceptibility; Kazumasa Hosoya, Masashi Takahashi and Takafumi Kitazawa measured and analyzed Mössbauer spectra; Kazumasa Hosoya and Shin-ichi Nishikiori performed all other experiments and analyses; and Takafumi Kitazawa wrote the paper.

Conflicts of Interest: The authors declare no conflict of interest.

References

1. Gütlich, P.; Hauser, A.; Spiering, H. Thermal and Optical Switching of Iron(II) Complexes. *Angew. Chem. Int. Ed. Engl.* **1994**, *33*, 2024–2054. [[CrossRef](#)]
2. Gütlich, P.; Goodwin, H.A. (Eds.) *Spin Crossover in Transition Metal Compounds I-III. Topics in Current Chemistry Vols. 233–235*; Springer: Berlin, Germany, 2004.
3. Muñoz, M.C.; Real, J.A. Thermo-, piezo-, photo- and chemo-switchable spin crossover iron(II)-metallocyanate based coordination polymers. *Coord. Chem. Rev.* **2011**, *255*, 2068–2093. [[CrossRef](#)]
4. Bousseksou, A.; Molnár, G.; Salmon, L.; Nicolazzi, W. Molecular spin crossover phenomenon: Recent achievements and prospects. *Chem. Soc. Rev.* **2011**, *40*, 3313–3335. [[CrossRef](#)] [[PubMed](#)]
5. Gütlich, P.; Gaspar, A.B.; Garcia, Y. Spin state switching in iron coordination compounds. *Beilstein J. Org. Chem.* **2013**, *9*, 342–391. [[CrossRef](#)] [[PubMed](#)]
6. Halcrow, M.A., Ed.; *Spin-Crossover Materials—Properties and Applications*; John Wiley & Sons: Chichester, UK, 2013.
7. Spenser, H.J.; Bartual-Murgui, C.; Molnár, G.; Real, J.A.; Muñoz, M.C.; Salmon, L.; Bousseksou, A. Thermal and pressure-induced spin crossover in a novel three-dimensional Hoffmann-like clathrate complex. *New J. Chem.* **2011**, *35*, 1205–1210. [[CrossRef](#)]
8. Sciortino, N.F.; Scherl-Gruenwald, K.R.; Chastanet, G.; Halder, G.J.; Chapman, K.W.; Létard, J.-F.; Kepert, C.J. Hysteretic Three-Step Spin Crossover in a Thermo- and Photochromic 3D Pillared Hofmann-type Metal-Organic Framework. *Angew. Chem. Int. Ed.* **2012**, *51*, 10154–10158. [[CrossRef](#)] [[PubMed](#)]
9. Arcís-Castillo, Z.; Muñoz, M.C.; Molnár, G.; Bousseksou, A.; Real, J.A. $[\text{Fe}(\text{TPT})_{2/3}[\text{M}^{\text{I}}(\text{CN})_2]] \cdot n\text{Solv}$ ($\text{M}^{\text{I}} = \text{Ag}, \text{Au}$): New Bimetallic Porous Coordination Polymers with Spin-Crossover Properties. *Chem. Eur. J.* **2013**, *19*, 6851–6861. [[CrossRef](#)] [[PubMed](#)]

10. Zhong, Z.J.; Tao, J.Q.; Yu, Z.; Dun, C.Y.; Liu, Y.J.; You, X.Z. A stacking spin-crossover iron(II) compound with a large hysteresis. *J. Chem. Soc. Dalton Trans.* **1998**. [[CrossRef](#)]
11. Létard, J.F.; Guionneau, P.; Rabardel, L.; Howard, J.A.K.; Goeta, A.E.; Chasseau, D.; Kahn, O. Structural, Magnetic, and Photomagnetic Studies of a Mononuclear Iron(II) Derivative Exhibiting an Exceptionally Abrupt Spin Transition. Light-Induced Thermal Hysteresis Phenomenon. *Inorg. Chem.* **1998**, *37*, 4432–4441. [[CrossRef](#)] [[PubMed](#)]
12. Gütlich, P.; Garcia, Y.; Goodwin, H.A. Spin crossover phenomena in Fe(II) complexes. *Chem. Soc. Rev.* **2000**, *29*, 419–427. [[CrossRef](#)]
13. Hayami, S.; Gu, Z.Z.; Shiro, M.; Einaga, Y.; Fujishima, A.; Sato, O. First Observation of Light-Induced Excited Spin State Trapping for an Iron(III) Complex. *J. Am. Chem. Soc.* **2000**, *122*, 7126–7127. [[CrossRef](#)]
14. Real, J.A.; Gaspar, A.B.; Niel, V.; Muñoz, M.C. Communication between iron(II) building blocks in cooperative spin transition phenomena. *Coord. Chem. Rev.* **2003**, *236*, 121–141. [[CrossRef](#)]
15. Real, J.A.; Gaspar, A.B.; Muñoz, M.C. Thermal, pressure and light switchable spin-crossover materials. *Dalton Trans.* **2005**. [[CrossRef](#)] [[PubMed](#)]
16. Scitortio, N.F.; Neville, S.M.; Létard, J.-F.; Moubaraki, B.; Murray, K.S.; Kepert, C.J. Thermal- and Light-Induced Spin-Crossover Bistability in a Disrupted Hofmann-Type 3D Framework. *Inorg. Chem.* **2014**, *53*, 7886–7893.
17. Klein, Y.M.; Sciortino, N.F.; Ragon, F.; Housecroft, C.E.; Kepert, C.J.; Neville, S.M. Spin crossover intermediate plateau stabilization in a flexible 2-D Hofmann-type coordination polymer. *Chem. Commun.* **2014**, *50*, 3838–3840. [[CrossRef](#)] [[PubMed](#)]
18. Powell, H.M.; Rayner, J.H. Clathrate Compound Formed by Benzene with an Ammonia-Nickel Cyanide Complex. *Nature* **1949**, *163*, 566–567. [[CrossRef](#)]
19. Rayner, J.H.; Powell, H.M. Structure of Molecular Compounds. Part X. Crystal Structure of the Compound of Benzene with an Ammonia-Nickel Cyanide. *J. Chem. Soc.* **1952**. [[CrossRef](#)]
20. Iwamoto, T.; Nakano, T.; Morita, M.; Miyoshi, T.; Miyamoto, T.; Sasaki, Y. The Hofmann-type Clathrate: $M(\text{NH}_3)_2M'(\text{CN})_4 \cdot 2\text{G}$. *Inorg. Chem. Acta* **1968**, *2*, 313–316. [[CrossRef](#)]
21. Iwamoto, T. The Hofmann-type and related inclusion compounds. In *Inclusion Compounds*; Atwood, J.L., Davies, J.E.D., MacNicol, D.D., Eds.; Academic Press: London, UK, 1984; Volume 1, pp. 29–57.
22. Akyüz, S.; Dempster, A.B.; Morehouse, R.L. An Infrared and Raman Spectroscopic Study of Some Metal Pyridine Tetracyanonickelate Complexes. *J. Mol. Struct.* **1973**, *17*, 105–125. [[CrossRef](#)]
23. Ülkü, D. Die Kristallstruktur des Dipyridin-cadmium tetracyanonickelats $\text{Cd}(\text{C}_5\text{H}_5\text{N})_2\text{Ni}(\text{CN})_4$. *Z. Kristallogr.* **1975**, *142*, 271–280.
24. Morehouse, R.L.; Aytaç, K.; Ülkü, D. Unit-cell dimension of Hofmann pyridine complexes. *Z. Kristallogr.* **1977**, *145*, 157–160. [[CrossRef](#)]
25. Kitazawa, T.; Gomi, Y.; Takahashi, M.; Enomoto, M.; Miyazaki, A.; Enoki, T. Spin-crossover behaviour of the coordination polymer $\text{Fe}(\text{C}_5\text{H}_5\text{N})_2\text{Ni}(\text{CN})_4$. *J. Mater. Chem.* **1996**, *6*, 119–121. [[CrossRef](#)]
26. Niel, V.; Martinez-Agudo, J.M.; Munoz, M.C.; Gaspar, A.B.; Réal, J.A. Cooperative Spin Crossover Behavior in Cyanide-Bridged Fe(II)-M(II) Bimetallic 3D Hofmann-like Networks (M = Ni, Pd, and Pt). *Inorg. Chem.* **2001**, *40*, 3838–3839. [[CrossRef](#)] [[PubMed](#)]
27. Tayagaki, T.; Galet, A.; Molnar, G.; Muñoz, M.C.; Zwick, A.; Tanaka, K.; Réal, J.A.; Bousseksou, A. Metal Dilution Effects on the Spin-Crossover Properties of the Three-Dimensional Coordination Polymer $\text{Fe}(\text{pyrazine})[\text{Pt}(\text{CN})_4]$. *J. Phys. Chem. B* **2005**, *109*, 14859–14867. [[CrossRef](#)] [[PubMed](#)]
28. Peng, H.; Tricard, S.; Félix, G.; Molnár, G.; Nicolazzi, W.; Salmon, L.; Bousseksou, A. Re-Appearance of Cooperativity in Ultra-Small Spin-Crossover $[\text{Fe}(\text{pz})\{\text{Ni}(\text{CN})_4\}]$ Nanoparticles. *Angew. Chem. Int. Ed.* **2014**, *53*, 10894–10898. [[CrossRef](#)] [[PubMed](#)]
29. Okabayashi, J.; Ueno, S.; Wakisaka, Y.; Kitazawa, T. Temperature-dependence EXAFS study for spin crossover complex: $\text{Fe}(\text{pyridine})_2\text{Ni}(\text{CN})_4$. *Inorg. Chim. Acta.* **2015**, *426*, 142–145. [[CrossRef](#)]
30. Muñoz-Páez, A.; Díaz-Moreno, S.; Marcos, E.S.; Rehr, J.J. Importance of Multiple-Scattering Phenomena in XAS Structural Determinations of $[\text{Ni}(\text{CN})_4]^{2-}$ in Condensed Phases. *Inorg. Chem.* **2000**, *39*, 3784–3790. [[CrossRef](#)] [[PubMed](#)]
31. Miyoshi, T.; Iwamoto, T.; Sasaki, Y. The Infrared Spectra of the Diamminemetal(II) Tetracyanonickelate(II) Benzene and Aniline Clathrates. *Inorg. Chem. Acta* **1967**, *1*, 120–126. [[CrossRef](#)]

32. Akyüz, S.; Dempster, A.B.; Morehouse, R.L. Host-guest interactions and stability of Hofmann-type benzene and aniline clathrates studied by i.r. spectroscopy. *Spectrochim. Acta* **1974**, *30A*, 1989–2004. [[CrossRef](#)]
33. Iwamoto, T.; Miyoshi, T.; Miyamoto, T.; Sasaki, Y.; Fujiwara, S. The Metal Ammine Cyanide Aromatic Clathrates. I. The Preparation and Stoichiometry of the Diamminemetal(II) Tetracyanonickelate(II) Dibenzene and Dianiline. *Bull. Chem. Soc. Jpn.* **1967**, *40*, 1174–1178. [[CrossRef](#)]
34. Matouzenko, G.S.; Molnar, G.; Bréfuel, N.; Perrin, M.; Bousseksou, A.; Borshch, S.A. Spin-Crossover Iron(II) Coordination Polymer with Zigzag Chain Structure. *Chem. Mater.* **2003**, *15*, 550–556. [[CrossRef](#)]
35. Southon, P.D.; Liu, L.; Fellows, E.A.; Price, D.J.; Halder, G.J.; Chapman, K.W.; Moubaraki, B.; Murray, K.S.; Létard, J.-F.; Kepert, C.J. Dynamic Interplay between Spin-Crossover and Host-Guest Function in a Nanoporous Metal-Organic Framework Material. *J. Am. Chem. Soc.* **2009**, *131*, 10998–11009. [[CrossRef](#)] [[PubMed](#)]
36. Ohba, M.; Yoneda, K.; Agustí, G.; Muñoz, M.C.; Gaspar, A.B.; Real, J.A.; Yamasaki, M.; Ando, H.; Nakao, Y.; Sakaki, S.; *et al.* Bidirectional Chemo-Switching of Spin State in a Microporous Framework. *Angew. Chem. Int. Ed.* **2009**, *48*, 4767–4771. [[CrossRef](#)] [[PubMed](#)]
37. Funasako, Y.; Mochida, T.; Takahashi, K.; Sakurai, T.; Ohta, H. Vapochromic Ionic Liquids from Metal-Chelate Complexes Exhibiting Reversible Changes in Color, Thermal, and Magnetic Properties. *Chem.-A Eur. J.* **2012**, *18*, 11929–11936. [[CrossRef](#)] [[PubMed](#)]
38. Wenger, O.S. Vapochromism in Organometallic and Coordination Complexes: Chemical Sensors for Volatile Organic Compounds. *Chem. Rev.* **2013**, *113*, 3686–3733. [[CrossRef](#)] [[PubMed](#)]
39. Jobbagy, C.; Deak, A. Stimuli-Responsive Dynamic Gold Complexes. *Eur. J. Inorg. Chem.* **2014**, *27*, 4434–4449. [[CrossRef](#)]
40. Kobayashi, A.; Kato, M. Vapochromic Platinum(II) Complexes: Crystal Engineering toward Intelligent Sensing Devices. *Eur. J. Inorg. Chem.* **2014**, *27*, 4469–4483. [[CrossRef](#)]
41. Naik, A.D.; Robeyns, K.; Meunier, C.F.; Léonard, A.F.; Rotaru, A.; Tinant, B.; Filinchuk, Y.; Su, B.L. Garcia Selective and Reusable Iron(II)-Based Molecular Sensor for the Vapor-Phase Detection of Alcohol. *Inorg. Chem.* **2014**, *53*, 1263–1265. [[CrossRef](#)] [[PubMed](#)]
42. Hosoya, K.; Kitazawa, T.; Takahashi, M.; Takeda, M.; Meunier, J.-F.; Molnár, G.; Bousseksou, A. Unexpected isotope effect on the spin transition of the coordination polymer $\text{Fe}(\text{C}_5\text{H}_5\text{N})_2[\text{Ni}(\text{CN})_4]$. *Phys. Chem. Chem. Phys.* **2003**, *5*, 1682–1688. [[CrossRef](#)]
43. Weber, B.; Bauer, W.; Pfaffeneder, T.; Dîrute, M.M.; Naik, A.D.; Rotaru, A.; Garcia, Y. Influence of Hydrogen Bonding on the Hysteresis Width in Iron(II) Spin-Crossover Complexes. *Eur. J. Inorg. Chem.* **2011**, *2011*, 3193–3206. [[CrossRef](#)]
44. Kitazawa, T.; Gomi, Y.; Takahashi, M.; Takeda, M. ^{57}Fe Mossbauer Spectra and Crystal Structure of Hofmann-type Thiophene Clathrate, $\text{Fe}(\text{NH}_3)_2\text{Ni}(\text{CN})_4 \cdot \text{C}_4\text{H}_4\text{S}$. *Mol. Cryst. Liq. Cryst.* **1998**, *311*, 167–172. [[CrossRef](#)]
45. Kitazawa, T.; Takahashi, M.; Takahashi, M.; Enomoto, M.; Miyazaki, A.; Enoki, T.; Takeda, M. ^{57}Fe Mossbauer Spectroscopic and Magnetic Study of the Spin-crossover Polymer Complex, $\text{Fe}(\text{3-Chloropyridine})_2\text{Ni}(\text{CN})_4$. *J. Radioanal. Nucl. Chem.* **1999**, *239*, 285–290. [[CrossRef](#)]
46. Molnár, G.; Guillon, T.; Moussa, N.O.; Rechinat, L.; Kitazawa, T.; Nardone, M.; Bousseksou, A. Two-step spin-crossover phenomenon under high pressure in the coordination polymer $\text{Fe}(\text{3-methylpyridine})_2[\text{Ni}(\text{CN})_4]$. *Chem. Phys. Lett.* **2006**, *423*, 152–156. [[CrossRef](#)]
47. Rodríguez-Velamazán, J.A.; Castro, M.; Palacios, E.; Burriel, R.; Kitazawa, T.; Kawasaki, T. A Two-Step Spin Transition with a Disordered Intermediate State in a New Two-Dimensional Coordination Polymer. *J. Phys. Chem. B* **2007**, *111*, 1256–1261. [[CrossRef](#)] [[PubMed](#)]
48. Kitazawa, T.; Takahashi, M.; Kawasaki, T. 2D iron(II) spin crossover complex with 3,5-lutidine. *Hyperfine Interact.* **2013**, *218*, 133–138. [[CrossRef](#)]
49. Kitazawa, T.; Takahashi, M. New Hofmann-like spin crossover compound with 3,5-lutidine. *Hyperfine Interact.* **2014**, *226*, 27–34. [[CrossRef](#)]
50. Sugaya, A.; Ueno, S.; Okabayashi, J.; Kitazawa, T. Crystal structure and magnetic properties of the spin crossover complex $\text{Fe}^{\text{II}}(\text{ethyl nicotinate})_2[\text{Au}^{\text{I}}(\text{CN})_2]_2$. *New J. Chem.* **2014**, *38*, 1955–1958. [[CrossRef](#)]
51. Ueno, S.; Kawasaki, T.; Okabayashi, J.; Kitazawa, T. Structural, Electronic, and Magnetic Properties of Novel Spin-Crossover Complex: $\text{Fe}(\text{butyl nicotinate})_2[\text{Au}(\text{CN})_2]_2$. *Bull. Chem. Soc. Jpn.* **2015**, *88*, 551–553. [[CrossRef](#)]

52. Ravel, B.; Newville, M. ATHENA, ARTEMIS, HEPHAESTUS: Data analysis for X-ray absorption spectroscopy using IFEFFIT. *J. Synchrotron Rad.* **2005**, *12*, 537–541. [[CrossRef](#)] [[PubMed](#)]
53. Ankudinov, A.L.; Ravel, B.; Rehr, J.J.; Conradson, S.D. Real-space multiple-scattering calculation and interpretation of X-ray-absorption near-edge structure. *Phys. Rev. B* **1998**, *58*, 7565–7566. [[CrossRef](#)]
54. Real, J.A.; Andrés, E.; Muñoz, M.C.; Julve, M.; Granier, T.; Bousseksou, A.; Varret, F. Spin Crossover in a Catenane Supramolecular System. *Science* **1995**, *268*, 265–267. [[CrossRef](#)] [[PubMed](#)]
55. Halder, G.J.; Kepert, C.J.; Moubaraki, B.; Murray, K.S.; Cashion, J.D. Guest-Dependent Spin Crossover in a Nanoporous Molecular Framework Material. *Science* **2002**, *298*, 1762–1765. [[CrossRef](#)] [[PubMed](#)]
56. Neville, S.M.; Moubaraki, B.; Murray, K.S.; Kepert, C.J. A thermal spin transition in a nanoporous iron(II) coordination framework material. *Angew. Chem. Int. Ed.* **2007**, *46*, 2059–2062. [[CrossRef](#)] [[PubMed](#)]
57. Seredyuk, M.; Gaspar, A.B.; Ksenofontov, V.; Reiman, S.; Galyametdinov, Y.; Haase, W.; Rentschler, E.; Gütllich, P. Multifunctional materials exhibiting spin crossover and liquid-crystalline properties. *Hyperfine Interact.* **2005**, *166*, 385–390. [[CrossRef](#)]
58. Niel, V.; Thompson, A.L.; Muñoz, M.C.; Galet, A.; Goeta, A.E.; Réal, J.A. Crystalline-state reaction with allosteric effect in spin-crossover, interpenetrated networks with magnetic and optical bistability. *Angew. Chem. Int. Ed.* **2003**, *42*, 3760–3763. [[CrossRef](#)] [[PubMed](#)]
59. Real, J.A.; Muñoz, M.C.; Andrés, E.; Granier, T.; Gallois, B. Spin-Crossover Behavior in the Fe(tap)₂(NCS)₂·nCH₃CN System (tap = 1,4,5,8-Tetraazaphenanthrene; n = 1, 1/2). Crystal Structures and Magnetic Properties of Both Solvates. *Inorg. Chem.* **1994**, *33*, 3587–3594. [[CrossRef](#)]
60. Hostettler, M.; Törnroos, K.W.; Chernyshov, D.; Vangdal, B.; Bürgi, H.-B. Challenges in engineering spin crossover: Structures and magnetic properties of six alcohol solvates of iron(II) tris(2-picolylamine) dichloride. *Angew. Chem. Int. Ed.* **2004**, *43*, 4589–4594. [[CrossRef](#)] [[PubMed](#)]
61. Bartel, M.; Absmeier, A.; Jameson, G.N.L.; Werner, F.; Kato, K.; Takata, M.; Boča, R.; Hasegawa, M.; Mereiter, K.; Caneschi, A.; *et al.* Modification of Spin Crossover Behavior through Solvent Assisted Formation and Solvent Inclusion in a Triply Interpenetrating Three-Dimensional Network. *Inorg. Chem.* **2007**, *46*, 4220–4229. [[CrossRef](#)] [[PubMed](#)]
62. Bartual-Murgui, C.; Salmon, L.; Akou, A.; Ortega-Villar, N.A.; Shepherd, H.J.; Muñoz, M.C.; Molnár, G.; Real, J.A.; Bousseksou, A. Synergetic Effect of Host-Guest Chemistry and Spin Crossover 3D Hofmann-like Metal-organic Frameworks [Fe(bpac)M(CN)₄] (M = Pt, Pd, Ni). *Chem. Eur. J.* **2012**, *18*, 507–516. [[CrossRef](#)] [[PubMed](#)]
63. Li, J.-Y.; He, C.-T.; Chen, Y.-C.; Zhang, Z.-M.; Liu, W.; Ni, Z.-P.; Tong, M.-L. Tunable cooperativity in a spin-crossover Hoffman-like metal-organic framework material by aromatic guests. *J. Mater. Chem. C* **2015**, *3*, 7830–7835. [[CrossRef](#)]
64. Kosone, T.; Kitazawa, T. Guest-dependent spin transition with long range intermediate state for 2-dimensional Hofmann-like coordination polymer. *Inorg. Chim. Acta.* **2016**, *439*, 159–163. [[CrossRef](#)]

